

Cottontail Rabbit Papillomavirus E8 Protein Is Essential for Wart Formation and Provides New Insights into Viral Pathogenesis

Mathieu Nonnenmacher,¹ Jérôme Salmon,¹† Yves Jacob,^{1,2} Gérard Orth,^{1*} and Françoise Breitburd^{1,2}

Unité des Papillomavirus¹ and Unité Génétique Papillomavirus et Cancer Humain,² Institut Pasteur, 75724 Paris Cedex 15, France

Received 11 December 2005/Accepted 27 February 2006

The cottontail rabbit papillomavirus (CRPV) a and b subtypes display a conserved E8 open reading frame encoding a 50-amino-acid hydrophobic protein, with structural similarities to the E5 transmembrane oncoprotein of genital human PVs (HPVs). CRPV E8 has been reported to play a role in papilloma growth but not to be essential in papilloma formation. Here we report that the knockout of E8 start codon almost prevented wart induction upon biobalistic inoculation of viral DNA onto rabbit skin. The scarce warts induced showed very slow growth, despite sustained expression of E6 and E7 oncogenes. This points to an essential role of E8 in disturbing epidermal homeostasis. Using a yeast two-hybrid screen, we found that E8 interacted with the zinc transporter ZnT1, protocadherin 1 (PCDH1), and AHNAK/desmoyokin, three proteins as yet unrelated to viral pathogenesis or cell transformation. HPV16 E5 also interacted with these proteins in two-hybrid assay. CRPV E8 mainly localized to the Golgi apparatus and the early endosomes of transfected keratinocytes and colocalized with ZnT1, PCDH1, and AHNAK. We showed that ZnT1 and PCDH1 formed a complex and that E8 disrupted this complex. CRPV E8, like HPV16 E5, increased epidermal growth factor (EGF)-dependent extracellular signal-regulated kinase 1/2 (ERK1/2) phosphorylation and both the EGF-dependent and the EGF-independent activity of activating protein-1 (AP-1). Competition experiments with a nonfunctional truncated ZnT1 protein showed that E8-ZnT1 interaction was required for AP-1 activation. Our data identify CRPV E8 as a key player in papilloma induction and unravel novel cellular targets for inducing the proliferation of keratinocytes.

Papillomaviruses (PVs) are small DNA viruses that induce cutaneous and mucosal epithelial proliferations in animals and humans. These lesions usually regress, but those associated with a subset of PVs may persist and progress into invasive carcinomas. The Shope cottontail rabbit papillomavirus (CRPV) induces skin warts and carcinomas in domestic rabbits (50). Among human PVs (HPVs), HPV5 is associated with flat wart-like lesions and carcinomas of the skin in patients suffering from epidermodysplasia verruciformis (47), and genital high-risk HPVs, mainly HPV16 and -18, cause anogenital intraepithelial lesions and are responsible for the vast majority of carcinomas of the uterine cervix (64). PVs contain two main oncogenes, E6 and E7, that are essential for epithelial proliferation and vegetative viral DNA replication. Both play a central role in the malignant progression of lesions associated with high-risk genotypes (for reviews, see references 10 and 44). High- and low-risk genital HPVs encode also an E5 oncoprotein with weak transforming activity in vitro. HPV E5 are short hydrophobic proteins associated with intracellular membranes that upregulate the mitogen-activated protein kinase (MAPK) signal cascade initiated by the epidermal growth factor (EGF) receptor (reviewed in reference 20) and increase the transcription of *jun* and *fos* early response genes in both EGF-dependent and EGF-independent manners (7, 14, 40). The E5 gene

is considered as no longer expressed in most cervical cancers, although recent evidence points to the expression of E5 protein in squamous cell carcinomas harboring episomal HPV16 genomes (13). The function of HPV E5 in vivo remains poorly understood (20), contrasting with the well-characterized E5 protein of bovine papillomavirus type 1 (BPV1), a virus that causes fibropapillomas in cattle and is capable of inducing cell transformation in vitro. E5 is the major BPV1 transforming gene in transformed cells and is believed to be responsible for the proliferation of dermal fibroblasts in vivo (33).

The CRPV constitutes the most amenable model to analyze the function of PV genes in vivo (10). CRPV is unlikely to encode a functional E5 protein (9, 51, 62) but displays an E8 open reading frame (ORF) (28) with a coding potential for a 50-amino-acid protein structurally related to the E5 protein encoded by BPV1 and genital HPVs (31). CRPV E8 shows little, if any, transforming activity in vitro (31) but has been reported to induce anchorage-independent growth of rodent cell lines in the presence of platelet-derived growth factor (PDGF) (30). The E8 protein has been shown to induce protective immunity against virus challenge in rabbits and has been reported to play a role in papilloma growth but not to be essential for papilloma formation (34).

Here we report for the first time that E8-knockout CRPV genomes display a dramatically reduced ability to induce skin papillomas in rabbits, which indicates that E8 provides an essential function in papilloma formation. We found that E8 interacted with the zinc transporter ZnT1, protocadherin 1 (PCDH1), and AHNAK/desmoyokin, three cellular proteins with no clear functional relationship and not yet related to viral infections or cell transformation. We observed that ZnT1

* Corresponding author. Mailing address: Département de Virologie, Institut Pasteur, 25 Rue du Dr Roux, F-75724 Paris, Cedex 15, France. Phone: 33 1 40 61 30 06. Fax: 33 1 45 68 89 66. E-mail: gorth@pasteur.fr.

† Present address: The Johns Hopkins University School of Medicine, Department of Pharmacology and Molecular Sciences, 725 North Wolfe Street, Baltimore, MD 21205.

formed a stable complex with PCDH1 and that E8 disrupted this complex. Like HPV16 E5, E8 localized to intracellular membranes and upregulated EGF-induced MAPK signaling and AP-1 activation when transiently expressed in cultured cells. We present experimental evidence for the requirement of E8-ZnT1 interaction in AP-1 overactivation. HPV16 E5 shared the same cellular targets as CRPV E8, suggesting similar pathogenic mechanisms.

MATERIALS AND METHODS

Recombinant CRPV genomes. The CRPVa4 and CRPVb recombinant plasmids were described previously (51, 52). A subgenomic 2.7-kb *EspI/SacI* fragment containing the long regulatory region and the E6, E8, and E7 ORFs was subcloned in the pBluescript plasmid (Stratagene) as previously reported (51). Site-directed mutagenesis of E8 initiation codon (ATG>ACG) was performed on subclones with the QuikChange Site-Directed Mutagenesis Kit (Stratagene), using complementary oligodeoxynucleotides (5'-CTGCAGGTCCCGTACGGC CACCC-3' and 5'-GGGTGGCCGTACGGGACCTGCAG-3') introducing a T>C mutation (underlined) at the nucleotide position 324 of CRPV. Mutant subclones were sequenced on both strands and ligated to the 5.2-kb homologous E1-L1 fragment of CRPVa or CRPVb to reconstitute full-length genomes, as previously described (51). Viral DNAs excised from plasmidic sequences and circularized were inoculated to five outbred New Zealand White rabbits with the Helios gene gun system (Bio-Rad) as previously described (51). Three animals were immunosuppressed during the whole experiment with methylprednisolone (43).

Tissue specimens and RNA analysis. Wart specimens were collected between 3 and 20 weeks after outgrowth, and were snap-frozen in liquid nitrogen for reverse transcription-PCR (RT-PCR) experiments or fixed in formalin and paraffin embedded for in situ hybridization experiments. RT-PCR analysis was carried out on warts induced by the four genomes in the same rabbit, as well as two additional pairs of CRPVa and CRPVaE8(-) specimens from another rabbit. Poly(A)⁺ RNA extracted from mechanically disrupted frozen tissue were reverse transcribed with Superscript II reverse transcriptase (Gibco-BRL). Duplex PCRs were carried out for 25 cycles with primers specific for conserved regions of CRPV E6 (5'-CGCTCGCTAGAGAAGCTGCAGC-3' and 5'-CCA GACTGTCAAACGTTCTTGACG-3') or E7 (5'-GTATTCTGCTATCCTGT GCGC-3' and 5'-AGCGATGCGGATAGCAGTCG-3'), together with degenerate primers specific for the desmocollin 2 cDNA (5'-GGWGTAGTTAATGAAGCTC CAT-3' and 5'-TACCTTATGCCACTGCTRCTTC-3') used as an internal control. Amplification products were separated in a 2% agarose gel and band intensities were measured with the Kodak 1D Image Analysis Software (Kodak Digital Science). Mean values of E6 and E7 bands, normalized to the corresponding desmocollin 2 bands, were compared by using the paired nonparametric Wilcoxon test. Detection of E6 transcripts by RNA-RNA in situ hybridization was performed on five pairs of specimens obtained from warts induced by CRPVa and CRPVa E8(-) genomes in the same rabbits. Specimens were cut into 5- to 7- μ m sections, and E6 transcripts were hybridized with a ³⁵S-labeled CRPVa E6 riboprobe (nucleotides [nt] 151 to 1005), as previously described (51).

Yeast two-hybrid analysis. A HaCaT cDNA library cloned in the pACT2 yeast two-hybrid vector and yielding 2.5×10^6 independent inserts (Clontech) was transfected into the Y187 yeast strain (*MAT α ura3-52 his3-200 ade2-101 trp1-901 leu2-3,112, gal4D met-gal80D URA3::GAL1_{UAS}-GAL1_{TATA}-lacZ*) according to standard procedures (27). CRPVa E8 DNA was cloned into the Gal4-BD yeast two-hybrid vector pGBK-T7 (Clontech), and transfection was performed into AH109 yeast cells (*MAT α trp1-901 leu2-3,112 ura3-52 his3-200 gal4D gal80D LYS2::GAL1_{UAS}-GAL1_{TATA}-HIS3 GAL2_{UAS}-GAL2_{TATA}-ADE2 URA3::MEL1_{UAS}-MEL1_{TATA}-lacZ*) (Clontech). The GAL4-BD-E8 fusion protein was nontoxic and did not induce autonomous transactivation. A mating strategy was used for two-hybrid screening of the human keratinocyte cDNA library (24). [His⁺] colonies were tested for *LacZ* expression by using an X-Gal (5-bromo-4-chloro-3-indolyl- β -D-galactopyranoside) overlay protocol. Positive clones were analyzed by direct sequencing of PCR products obtained from colonies or by sequencing of plasmid DNA amplified in DH5 α bacteria.

Plasmid constructs. CRPVa and CRPVb E8 coding sequences (nt 323 to 472) were amplified by PCR and cloned into the XhoI/XbaI restriction sites of pCiNeo (Promega) and pEGFP-N1 (Clontech) vectors according to standard molecular biology techniques. A vesicular stomatitis virus (VSV)-tagged form of E8 was generated by using PCR by inserting a VSV-G epitope in the 5' E8

primer. The resulting PCR fragment was inserted into the pCiNeo vector. The MMP1-luc plasmid has been described previously (37) and was kindly provided by Fatima Mechta-Gregoriou (Institut Pasteur, Paris, France). All other constructs were obtained by recombinational cloning using Gateway technology (Invitrogen) according to the manufacturer's instructions. Briefly, CRPVa and CRPVb E8 were amplified by PCR with AttB-modified primers to allow insertion into gateway-modified pGBKT7 and pHcRed-N1 vectors (Clontech). Similarly, HPV16 E5 coding sequence (nt 3850 to 4101) was amplified from the prototypical HPV16 genome and inserted into pGBK-T7 and pCiNeo plasmids. ZnT1 full-length cDNA was obtained by RT-PCR from HaCaT total RNA and inserted into gateway-modified pEGFP-C1 plasmid (Clontech) or pCiNeo-Flag plasmid (modified from pCiNeo by insertion of an IBI triple flag sequence). Sequences encoding ZnT1 $_{\Delta 1-177}$, AHNAK $_{1660-2200}$, AHNAK $_{3926-5643}$, and PCDH $_{1620-1060}$ fragments and full-length PCDH1 were amplified from pACT2 clones isolated during the two-hybrid screen and cloned into gateway-modified pEGFP-C1 and pCiNeo-Flag vectors.

Immunoprecipitation and Western blot analysis. Transient expression of GFP- and flag-tagged proteins was achieved by calcium phosphate transfection of HEK-293T cells. Protein extracts were prepared in radioimmunoprecipitation assay buffer and immunoprecipitation was performed with Protein G Plus/Protein A-Agarose beads (Oncogene Research Products) previously coated with anti-flag M2 (Sigma) or anti-GFP (Clontech) antibody. Immunoprecipitates were then submitted to sodium dodecyl sulfate-polyacrylamide gel electrophoresis (SDS-PAGE) and immunoblotted with mouse anti-GFP monoclonal antibody (Mab; Clontech), mouse anti-Flag M2 Mab (Sigma), or rabbit anti-AHNAK (KIS) polyclonal antibody (a generous gift from Benoit Gentil, CEA, Grenoble, France), followed by peroxidase-conjugated anti-mouse or anti-rabbit secondary antibodies.

Fluorescence microscopy. HaCaT cells were plated on 18-mm glass coverslips and cultured in Eagle minimal essential medium (Gibco) supplemented with 10% fetal calf serum (FCS), 6.5 ng of EGF (Sigma)/ml, 2 mM L-glutamine, and 0.5 μ g of hydrocortisone/ml and antibiotics. Transfections were performed with high-molecular-weight polyethylenimine (Sigma) as previously described (6), and cells were fixed in 4% paraformaldehyde 24 h thereafter. The following primary antibodies were used: mouse anti-EEA1 Mab, mouse anti-Golgin-97 Mab, and mouse anti-GM130 Mab (all from Transduction Laboratories). For activated EGFR colocalization studies, HeLa cells were maintained in Dulbecco minimal essential medium (Gibco) supplemented with 10% FCS and antibiotics and cotransfected by calcium phosphate precipitation with E8-GFP plasmid, together with the EGFR-pRK5 plasmid (32), a generous gift from Sheila Harroch (Institut Pasteur, Paris, France). Cells were serum starved in 0.1% FCS medium for 24 h, incubated 5 min at 4°C with 100 ng of EGF/ml, and chased at 37°C for 15 or 30 min. Activated EGFR was visualized by indirect immunofluorescence with an anti-phospho-EGFR antibody (Transduction Laboratories). Coverslips were mounted in Vectashield or Vectashield plus DAPI medium (Vector Laboratories) and examined under a Zeiss LSM 150 or Leica TC54D confocal microscope or under a Zeiss Axioplan 2 wide-field Apo Tome microscope.

Activation of MAPKs and AP-1 luciferase reporter assays. HEK-293T cells were maintained in Dulbecco modified Eagle medium supplemented with 10% FCS and antibiotics. To analyze the activation of the MAPK extracellular signal-regulated kinases 1 and 2 (ERK1/2), HEK-293T cells were transfected by calcium phosphate precipitation with pCiNeo, pCiNeo-E8, or pCiNeo-E5 plasmid and serum starved for 24 h. Cells were treated 10 min with 100 ng of EGF/ml and lysed in NP-40 buffer. Protein extracts were separated by SDS-PAGE, transferred on Hybond ECL nitrocellulose membranes (Amersham), and incubated with an antibody specific for the phosphorylated forms of ERK1/2 (Santa Cruz), followed by a peroxidase-conjugated anti-mouse antibody (Vector Labs). Proteins were visualized by chemiluminescence (Supersignal; Pierce). Membranes were reincubated with an antibody specific for α -tubulin (Upstate Biotechnology) to demonstrate equal loading.

For AP-1 reporter assays, HEK-293T cells were seeded on 12-well poly-L-lysine-coated plates and transfected with 1 μ g of each expression vector (the total amount of plasmid DNA was kept to 4 μ g by addition of pCiNeo), together with 1 μ g of MMP1-luc reporter plasmid and with 0.1 μ g of pEGFP-N1 as a transfection control. Cells were serum starved for 24 h and stimulated for 16 h with 20 ng of EGF/ml. Protein lysates were analyzed for luciferase activity with a Lumat LB 9507 luminometer (Berthold Technologies). Transfection efficiency was normalized by measuring GFP fluorescence of lysates with a multiwell Victor 2 fluorimeter (Wallac, Inc.). All experiments were performed in triplicate and repeated at least three times to ensure reproducibility. Mean values were compared by using the unpaired *t* test.

RESULTS

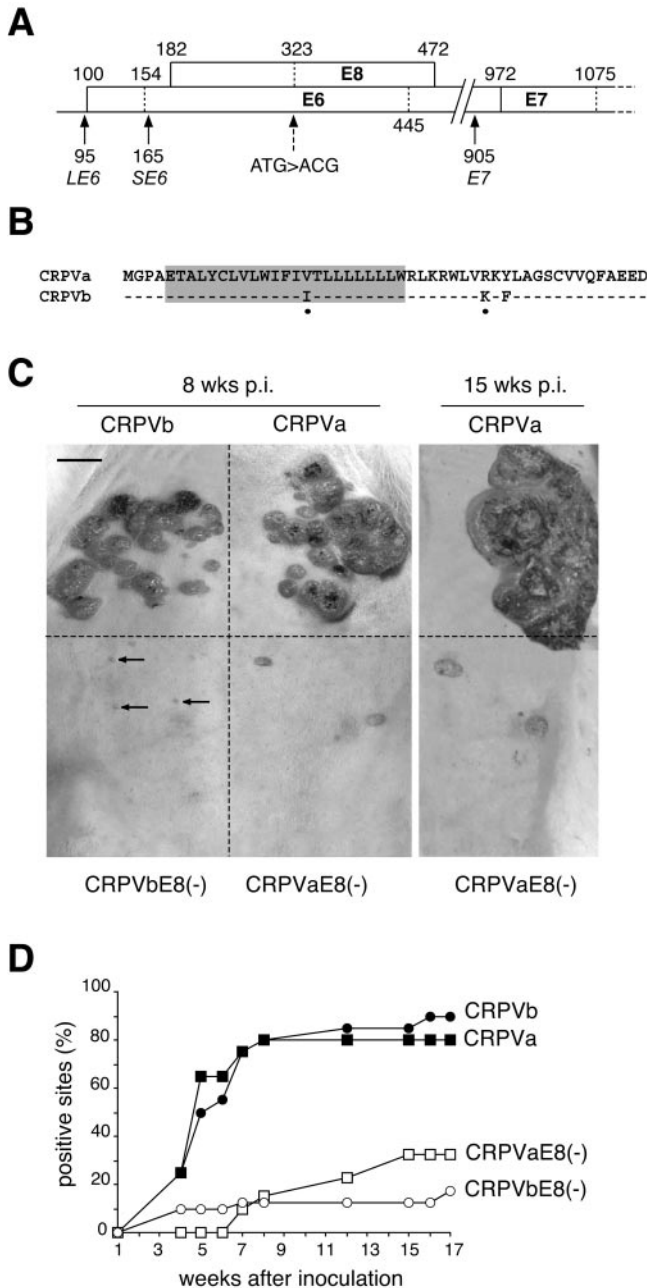


FIG. 1. Role of E8 in wart induction and growth. (A) Location of CRPV E8 ORF in the E6/E7 region. Open bars represent ORFs, and dashed lines indicate start codons. Transcription start sites of the long E6 (LE6), short E6 (SE6), and E7 transcripts (18) are indicated by solid arrows. Mutant E8(-) genomes were obtained by site-directed mutagenesis of the E8 start codon (dashed arrow). Nucleotide positions refer to the CRPVa4 sequence (51). (B) Amino acid sequence alignment of E8 proteins encoded by CRPVa and CRPVb. Dots indicate conservative amino acid changes. The shaded box indicates putative helical transmembrane domains, as predicted by the Transmembrane Hidden Markov Model software (version 2.0; <http://www.cbs.dtu.dk/services/TMHMM>). (C) Induction of warts by wt and E8(-) mutant CRPVa and CRPVb genomes. Genomes were inoculated with a gene gun at four sites (for wt genomes) and eight sites [for E8(-) genomes] per rabbit as described in Materials and Methods. Pictures show warts obtained in the same rabbit 8 and 15 weeks after inoculation. Bar, 1 cm. (D) Kinetics of wart induction after the inoculation of wt and mutant CRPVa and CRPVb genomes into five rabbits. The

CRPV E8 is required for the induction of warts. We previously characterized two CRPV subtypes (CRPVa and CRPVb) with highly divergent E6 and E7 ORFs and with distinct biological properties (51, 52). Both subtypes contain a conserved E8 ORF, colinear to the E6 reading frame, whose initiation codon lies in the 5' part of E6 transcripts (Fig. 1A). The E8 ORF encodes a 50-amino-acid hydrophobic protein with a 23-amino-acid putative transmembrane domain and with only three variable residues, including two conservative changes (Fig. 1B). In order to characterize the role of the E8 protein in CRPV biology, E8-knockout CRPVa and CRPVb genomes, referred to as E8(-), were generated by site-directed mutagenesis of the E8 initiation codon (Fig. 1A), without affecting the E6-encoded amino acid sequence (31). Mutant E8(-) and wild-type (wt) CRPV genomes were inoculated onto the dorsal skin of five outbred New Zealand White rabbits. Each animal received the two wt genomes (four sites each) and the two E8(-) genomes (eight sites each). Three rabbits were immunosuppressed with methylprednisolone (43) to prevent early wart regression (29, 51). Multiple warts (5 to 10 per inoculated site) developed within 4 to 8 weeks in all rabbits at most sites inoculated with wt CRPVa or CRPVb (80 and 90%, respectively) (Fig. 1C and D). In contrast, E8(-) CRPVa and CRPVb genomes induced only single warts (one or two per site) at fewer inoculated sites (32.5 and 17.5% positive sites), respectively, in only three of the five animals (two immunocompetent and one immunosuppressed rabbits). Early regression of CRPVb and CRPVb E8(-) warts was observed in one of the two immunocompetent rabbits, whereas no early regression was observed in immunosuppressed animals. Warts induced by wt genomes became large and confluent within 6 to 8 weeks after outgrowth, whereas the scarce warts induced by mutant genomes showed very slow or even abortive growth (Fig. 1C). These observations demonstrate that E8 is essential both for papilloma induction and for the growth of established warts.

Since E6 and E7 oncogenes are both required for wart formation (63), we examined whether impaired wart growth involved transcriptional downregulation of E6 or E7 genes. No significant difference was found for E6 and E7 expression level, as deduced from the band intensities of RT-PCR products (Fig. 2A), and no noticeable variation was observed in the level and distribution of E6 transcripts, as detected by in situ hybridization (Fig. 2B). Our data indicate that E8 provides an essential function to trigger the proliferation of epidermal cells.

CRPV E8 interacts with AHNAK, ZnT1, and PCDH1 in a yeast two-hybrid assay. As a general approach to address the mechanisms underlying the biological properties of E8, we searched for the cellular targets of E8 by yeast two-hybrid screening. CRPVa E8 (E8a) was taken as a bait to screen a cDNA library established from the HaCaT keratinocyte cell

total numbers of sites with warts were observed during a 17-week follow-up. The values reported on the y axis represent the percentage of total positive sites versus total inoculated sites.

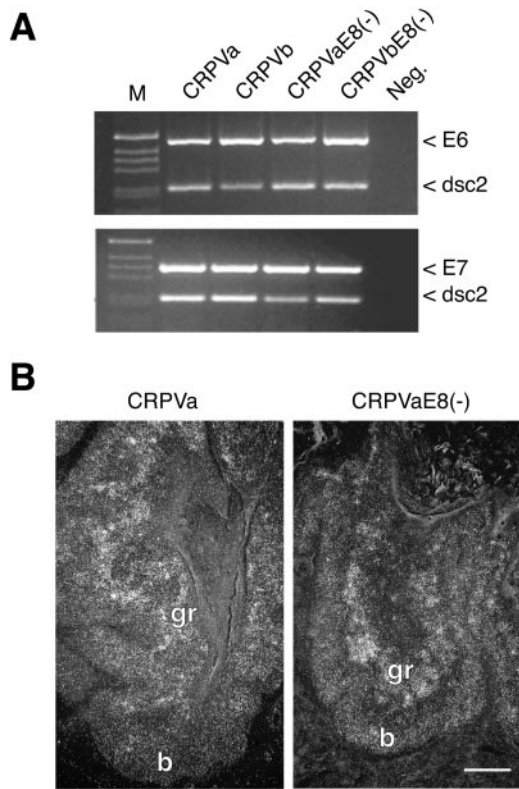


FIG. 2. Transcription of E6 and E7 oncogenes in warts induced by wt and E8(-) CRPV genomes. (A) RT-PCR analysis of E6 and E7 transcripts. Total RNA was extracted from warts collected in the same rabbit and reverse transcribed. PCRs were carried out with primers specific for E6 or E7 sequences, together with primers for the keratinocyte-specific desmocollin 2 (Dsc 2) cDNA. PCR products were separated on agarose gel and band intensities were estimated with the Kodak 1D Image Analysis Software (Kodak Digital Science). (B) Detection of E6 transcripts by in situ hybridization. Warts induced in the same rabbit by wild-type or mutant CRPVa genomes were processed for in situ hybridization with an E6-specific ³⁵S-labeled riboprobe. E6 expression pattern was similar in both lesions and characterized by a strong labeling in the basal and parabasal layers (b) and in the granular layer (gr). Bar, 100 μm.

line, using a two-hybrid mating assay (24). A total of 161 His⁺ clones were identified, and 82 were validated for interaction by a β-galactosidase overlay assay. Among these, 17 clones encoded partial cDNAs of the giant AHNAK protein (Swiss-Prot M80902, X74818) (57). This protein was first described as desmoyokin, a keratinocyte nondesmosomal plaque protein (41), but its function in skin homeostasis is still poorly understood (38). Of the three cDNA species identified, two encoded nonoverlapping segments composed exclusively of highly conserved repeated units (CRUs) of 128 amino acids (Fig. 3A). This indicates that AHNAK can bind several E8 molecules via its CRUs. Eleven clones encoded a segment of the ubiquitous zinc transporter ZnT1 (Swiss-Prot AF323590) (48) comprising the two C-terminal transmembrane domains and the C-terminal cytoplasmic domain, but not the N-terminal region required for its activity (48) (Fig. 3A). Five clones corresponded to the mRNA variant 1 of protocadherin 1 (PCDH1) (Swiss-Prot BC035812), encoding a still poorly characterized transmembrane protein, potentially involved in calcium-dependent

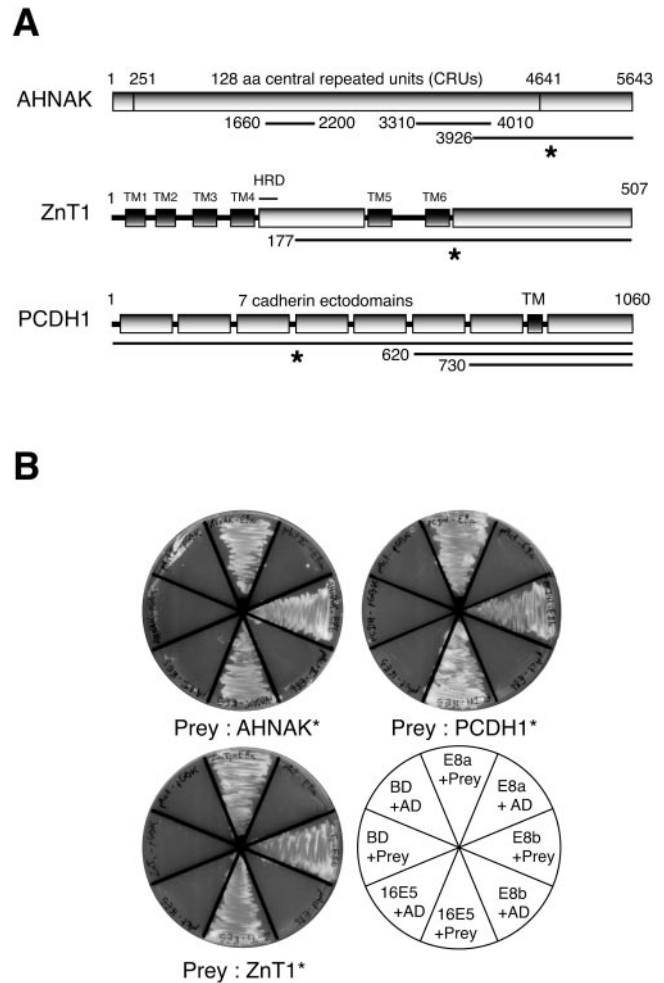


FIG. 3. Identification of CRPV E8-interacting proteins by yeast two-hybrid assay. (A) Schematic representation of the E8-interacting proteins identified by two-hybrid screening. Bars represent the sequences encoded by the clones identified in our assay. The 128-amino-acid central repeated units (CRUs) of AHNAK, the histidine-rich zinc-binding domain (HRD, amino acids 145 to 155) of ZnT1, the seven cadherin ectodomains of PCDH1, and the transmembrane domains (TM, dark shaded boxes) are indicated. (B) Confirmation of the interactions by pairwise two-hybrid assay. CRPVa E8 (E8a), CRPVb E8 (E8b), and HPV16 E5 (16E5), linked to the Gal4 DNA-binding domain (BD), were used as baits to test for interaction with each prey fused to the Gal4 activation domain (AD) on -His medium. Preys correspond to the clones marked with an asterisk in panel A, and empty vectors were used as controls, as depicted in the scheme.

cell-cell adhesion and signal transduction (22, 53, 59). The shortest PCDH1 clone isolated in the screen (residues 730 to 1060) defined a C-terminal region comprising one cadherin-like ectodomain, as well as the transmembrane and cytoplasmic domains (Fig. 3A).

The specificity of the interactions between CRPV E8a and AHNAK, PCDH1, or ZnT1 proteins was confirmed by pairwise two-hybrid assay on -His medium (Fig. 3B). None of the three proteins showed nonspecific Gal4 transactivation when cotransfected with a vector encoding the Gal4 DNA-binding domain (BD) alone (Fig. 3B). The CRPVb E8 (E8b) showed the same interactions as the CRPVa E8 protein. In view of the

structural similarities of CRPV E8 and HPV E5 proteins, we looked for specific interactions between the HPV16 E5 protein and the cellular partners of E8. Most interestingly, HPV16 E5 showed specific binding to each of the three E8-interacting proteins in this assay (Fig. 3B). To our knowledge, no relationship has been reported between AHNAK, PCDH1, and ZnT1, and none of these proteins has been previously linked to viral pathogenesis or cell transformation.

CRPV E8 binds to AHNAK, ZnT1, and PCDH1 in mammalian cell extracts. Coimmunoprecipitation experiments were performed to demonstrate that E8 could interact with AHNAK, PCDH1, and ZnT1 proteins in mammalian cells. Human embryonic kidney (HEK) 293T cells were cotransfected with E8-GFP or GFP plasmid together with flag-AHNAK, flag-PCDH1, or flag-ZnT1 plasmid. The flag-AHNAK fusion construct was obtained from the AHNAK fragment encoding amino acids 1660 to 2200, which contains only CRUs (Fig. 3A) and the flag-PCDH1 expression vector from the fragment encoding amino acids 620 to 1060 (Fig. 3A). Full-length ZnT1 cDNA was obtained by RT-PCR from HaCaT total RNA. In total cell extracts, flag-AHNAK₁₆₆₀₋₂₂₀₀ and flag-PCDH1₆₂₀₋₁₀₆₀ proteins were detected at 55 to 60 kDa and 45 to 50 kDa, respectively (Fig. 4A, left panel), as expected from their calculated molecular mass (59 and 48 kDa, respectively). The flag-ZnT1 protein showed an apparent molecular mass (35–40 kDa) lower than expected (56 kDa), in agreement with previous observations (42) (Fig. 4A, left panel). Cell lysates were immunoprecipitated with an anti-GFP antibody and precipitates were immunoblotted with an anti-flag antibody. E8-GFP was able to coimmunoprecipitate each of AHNAK₁₆₆₀₋₂₂₀₀, PCDH1₆₂₀₋₁₀₆₀, and full-length ZnT1 (Fig. 4A, right panel). No interaction was observed in control cells expressing GFP alone. Conversely, the E8-GFP protein was detected in the anti-flag immunoprecipitates obtained from cells expressing flag-ZnT1, flag-PCDH1₆₂₀₋₁₀₆₀, or flag-AHNAK₁₆₆₀₋₂₂₀₀ plasmid (Fig. 4B). No E8-GFP was detected in the immunoprecipitates from control cells expressing no flag-tagged protein or an irrelevant flagged protein (flag-NECAB) (Fig. 4B). Direct interaction of CRPV E8 with endogenous AHNAK could also be demonstrated by immunoprecipitation with an anti-AHNAK antibody (anti-KIS [described in reference 56]) (data not shown). These results demonstrate that E8 physically interacts with ZnT1, PCDH1, and AHNAK proteins in mammalian cells.

CRPV E8 colocalizes with AHNAK, PCDH1, and ZnT1 in cytoplasmic vesicles. Confocal analysis of transiently transfected keratinocytes was performed to identify the subcellular localization of E8 and to determine whether E8 colocalizes with its targets. CRPV E8 subcellular localization was analyzed in HaCaT cells transiently transfected with a E8-GFP fusion construct. Confocal analysis showed a strong labeling of cytoplasmic vesicles, mainly in the perinuclear area, and a weaker labeling of the plasma membrane (Fig. 5). Complete colocalization was observed between E8-GFP and VSV-E8 fusion proteins (data not shown), thus indicating that the length or the C-terminal or N-terminal position of the tag had no effect on the subcellular localization of the protein. No overlapping was observed between E8-GFP and markers specific for the endoplasmic reticulum (calnexin) or late endosomes (LAMP-1) (data not shown). The distribution of E8 partially overlapped the cis/medial and trans-Golgi networks,

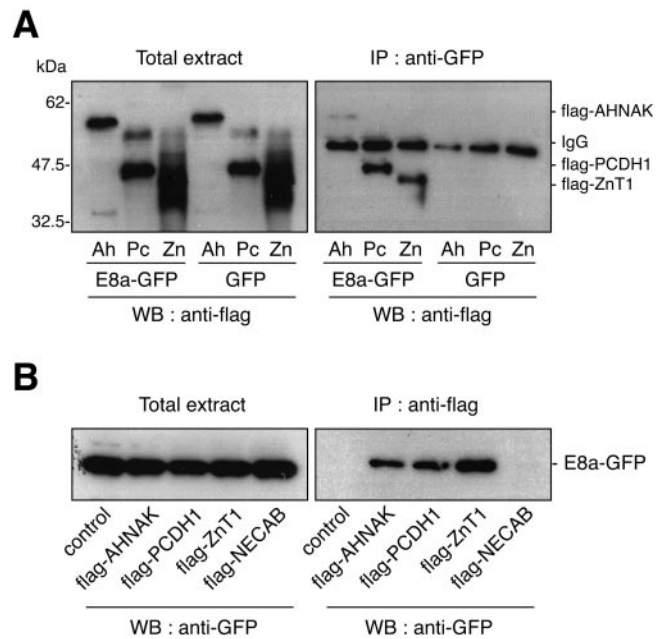


FIG. 4. Coimmunoprecipitation of E8 with AHNAK, PCDH1, or ZnT1. (A) HEK-293T cells were cotransfected with recombinant pCNeo vectors encoding CRPV E8-GFP (E8a-GFP) or GFP alone, together with vectors encoding flag-AHNAK₁₆₆₀₋₂₂₀₀ (Ah), flag-PCDH1₆₂₀₋₁₀₆₀ (Pc), or flag-ZnT1 (Zn). Protein extracts were subjected to immunoprecipitation (IP) with an anti-GFP antibody. Total cell extracts and immunoprecipitates were run on SDS-PAGE gels, transferred onto nitrocellulose membranes, and probed with an anti-flag antibody (WB, anti-flag). IgG, immunoglobulin heavy chain. (B) HEK-293T cells were cotransfected with E8a-GFP plasmid, together with flag-AHNAK₁₆₆₀₋₂₂₀₀, flag-PCDH1₆₂₀₋₁₀₆₀, or flag-ZnT1 plasmid. Control cells were transfected with E8a-GFP vector alone or with a plasmid encoding the irrelevant flag-NECAB fusion protein. Anti-flag immunoprecipitation was performed, and total extracts and immunoprecipitates (IP) were immunoblotted with an anti-GFP antibody (WB, anti-GFP).

stained with antibodies to GM130 (Golgi Matrix protein 130) and golgin 97, respectively (Fig. 5). Partial colocalization was also observed with early endosomes, as revealed by using an antibody to early endosome antigen 1 (EEA1). Of note, a similar subcellular localization pattern was reported previously for HPV16 and HPV2a E5 proteins (12, 46).

For colocalization experiments, full-length PCDH1 and ZnT1 cDNAs were used to generate green fluorescent protein (GFP) fusion constructs. Due to the unusually large size of AHNAK coding sequence (16.9 kb), a fusion construct was obtained from a fragment encoding amino acids 3926 to 5643 (Fig. 3A), which contains the C-terminal domain required for proper AHNAK subcellular localization (45). HaCaT cells were cotransfected with an E8a-hcRed construct (red fluorescence), together with GFP-AHNAK₃₉₂₆₋₅₆₄₃, GFP-PCDH1, or GFP-ZnT1 construct (green fluorescence). Each of the three E8-interacting proteins showed colocalization with E8 (yellow staining), mainly in cytoplasmic and perinuclear vesicles (Fig. 5).

CRPV E8 releases ZnT1 from a complex involving PCDH1. No functional relationship has been reported thus far between AHNAK, PCDH1, and ZnT1. We sought to determine whether these proteins could be part of a common complex. Immuno-

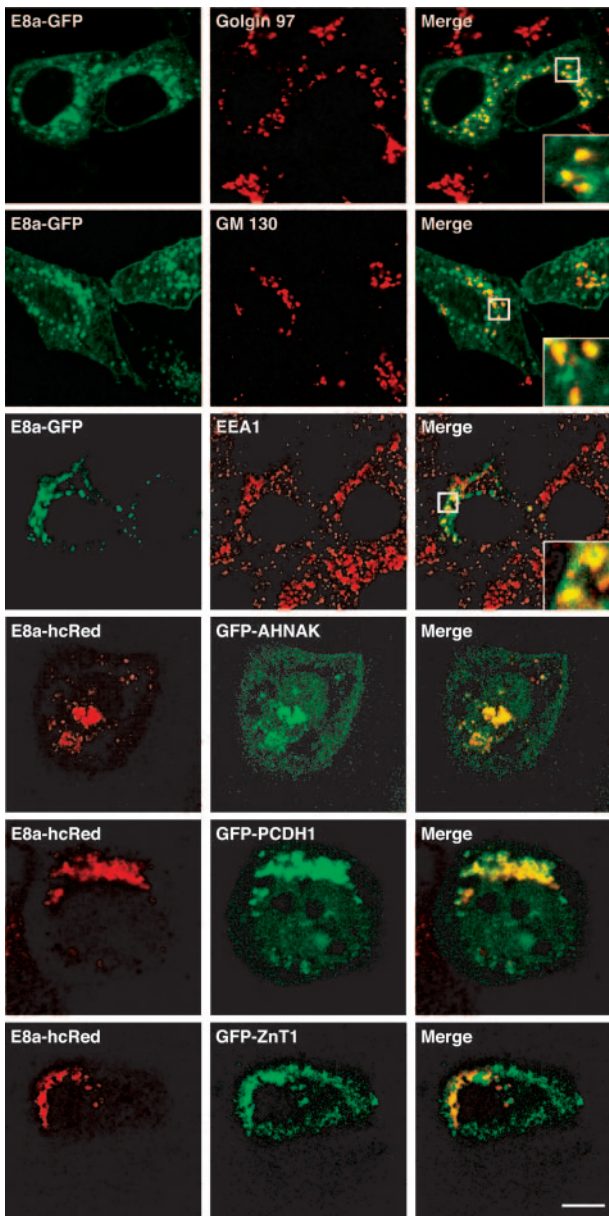


FIG. 5. Localization of CRPV E8 and its targets in keratinocytes. HaCaT cells were transfected with CRPVa E8-GFP (E8a-GFP) vector (upper panels) or cotransfected with a CRPVa E8-hcRed expression plasmid (E8a-hcRed) together with a GFP-AHNAK₃₉₂₆₋₅₆₄₃, GFP-PCDH1, or GFP-ZnT1 expression vector (lower panels). Cells were fixed 24 h after transfection and stained with antibodies specific for the trans-Golgi network (anti-golgin-97), cis/medial Golgi (anti-GM130), and early endosomes (anti-EEA1), followed by a Cy3-conjugated secondary antibody (upper panels). Fluorescence emissions were imaged by laser-scanning confocal microscopy. Insets show a higher magnification of boxed areas. Bar, 10 μ m.

precipitation experiments were performed after cotransfection of HEK-293T cells with plasmids encoding flagged full-length PCDH1 and GFP-tagged full-length ZnT1. The AHNAK-specific antibody anti-KIS (56) was used to detect endogenous AHNAK protein (Fig. 6A). No interaction was observed between AHNAK and PCDH1 or between AHNAK and ZnT1 (Fig. 6A). In contrast, GFP-ZnT1 fusion protein was detected

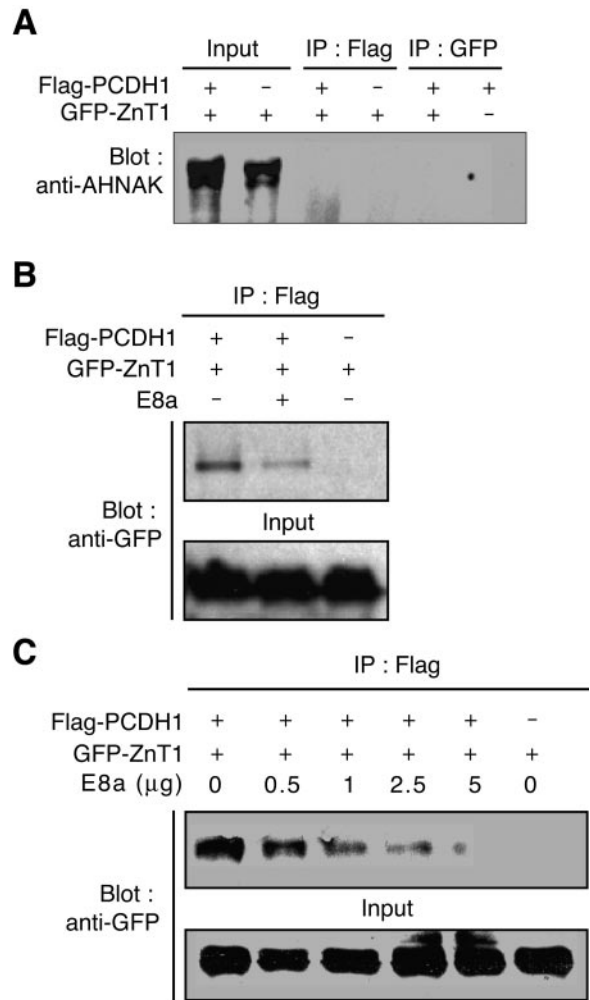


FIG. 6. Analysis of the interactions between AHNAK, PCDH1, and ZnT1. (A) Lack of interaction between endogenous AHNAK and PCDH1 or ZnT1. HEK-293T cells were cotransfected with flag-PCDH1 and/or GFP-ZnT1 constructs, lysed, and immunoprecipitated using an anti-flag or anti-GFP antibody. Whole-cell lysates and immunoprecipitates were immunoblotted with an antibody specific for AHNAK central repeated units (anti-KIS) that allowed detection of a band of high molecular weight in cell lysates. (B) Evidence for a ZnT1-PCDH1 complex. HEK 293T cells were cotransfected with flag-PCDH1 and GFP-ZnT1 plasmids or with flag-PCDH1, GFP-ZnT1, and CRPVa E8 (E8a) plasmids. Whole-cell lysates were immunoprecipitated with anti-flag antibody, and immunoprecipitates were immunoblotted with an anti-GFP antibody. Control cells were transfected with GFP-ZnT1 plasmid alone. (C) Dose-dependent disruption of ZnT1-PCDH1 complex by E8. HEK-293T cells were cotransfected with flag-PCDH1 and GFP-ZnT1 plasmids, together with various amounts of E8a plasmid. Flag immunoprecipitates were immunoblotted with anti-GFP antibody.

in flag-PCDH1 immunoprecipitates but not in immunoprecipitates obtained from control cells (Fig. 6B). Conversely, GFP-PCDH1 was detected as a faint band in flag-ZnT1 immunoprecipitates (data not shown).

We next sought to determine whether E8 could interfere with the formation of the ZnT1-PCDH1 complex. The amount of GFP-ZnT1 detected in flag-PCDH1 immunoprecipitates was reduced in the presence of E8 protein (Fig. 6B), and

cotransfection of cells with increasing amounts of E8-expressing vector showed that E8 inhibited ZnT1-PCDH1 interaction in a dose-dependent manner (Fig. 6C). These findings show for the first time that the ZnT1 and PCDH1 transmembrane proteins can form a complex, and establish that E8 interferes with ZnT1-PCDH1 interaction.

CRPV E8 enhances EGF-dependent and -independent signal transduction. Previous studies showed that HPV16 E5 enhances EGF-dependent ERK/MAPK signaling and increases the transcription of early response genes such as *c-jun* and *c-fos* in both EGF-dependent and EGF-independent manners (20). We first sought to determine whether CRPV E8 could potentiate EGF-dependent MAPK signaling. HEK-293T cells were transiently transfected with a construct expressing untagged CRPVa E8 or, as a control, the HPV16 E5 protein, and treated with EGF for 10 min. Cell extracts were then immunoblotted with an antibody specific for the active phosphorylated form of ERK1/2. CRPV E8 induced a marked increase in ERK1/2 phosphorylation upon EGF treatment, but no ERK1/2 activation was observed without ligand treatment (Fig. 7A). Similar results were obtained with cells transfected with the HPV16 E5 gene, in agreement with previous reports (12).

We next investigated to what extent E8 modulates the transcriptional activity of AP-1 Jun/Fos complexes by using a reporter construct encoding the luciferase gene driven by the AP-1 responsive element of the matrix metalloprotease 1 promoter (MMP1-luc). Cells expressing CRPVa E8 (E8a) or CRPVb E8 (E8b) protein showed a strong AP-1 activation after overnight treatment with EGF (11- and 11.2-fold, respectively) compared to EGF-treated control cells (Fig. 7B). Cells expressing HPV16 E5 protein (16 E5) showed a sevenfold AP-1 activation. Moderate AP-1 activation was observed in the absence of EGF treatment in cells expressing E8a (4.4-fold) or E8b (3.9-fold), as also observed in cells expressing HPV16 E5 (2.1-fold) (Fig. 7B). Together, these data indicate that CRPV E8 strongly enhances EGFR signaling to the nucleus but also leads to a moderate AP-1 activation through an EGF-independent signaling pathway.

E8-ZnT1 interaction is required for AP-1 activation. The *Caenorhabditis elegans* homologue of ZnT1, the cation diffusion facilitator 1, was recently identified as a positive modulator of EGFR signaling (11, 36). To assess whether E8-ZnT1 interaction was required for AP-1 activation, we performed competition experiments by overexpressing an E8-interacting nonfunctional form of ZnT1. Previous studies showed that the removal of the first 73 residues of ZnT1 created a nonfunctional protein that could not interfere with the activity of the endogenous protein (48). We used a fragment of ZnT1 lacking the first 177 residues (ZnT1 $_{\Delta 1-177}$). The resulting protein lacks the first four membrane-spanning domains but retains the E8-binding domain (Fig. 3A). AP-1 activity was assessed in HEK-293T cells transfected with either ZnT1 $_{\Delta 1-177}$ or full-length ZnT1 construct. Ectopic expression of full-length ZnT1 resulted in a moderate increase of AP-1 activity (3.2-fold) in response to EGF, whereas ZnT1 $_{\Delta 1-177}$ had no significant effect (Fig. 8A). E8 expression induced a strong (11-fold) AP-1 activation upon EGF treatment, as expected, and this activation was significantly increased after ectopic expression of full-length ZnT1 (13-fold versus 11-fold, $P < 0.05$ [*t* test]). In

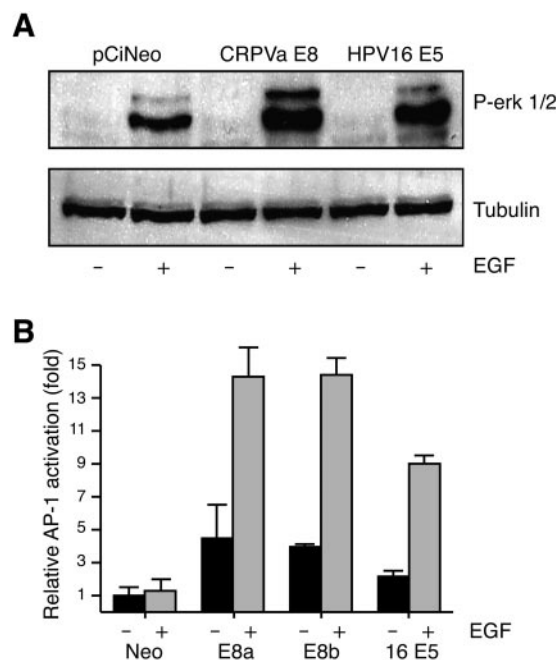


FIG. 7. Role of CRPV E8 in ERK1/2 and AP-1 activation. (A) Effect of E8 on ERK1/2 activation. HEK-293T cells were transfected with recombinant pCiNeo vectors encoding untagged CRPVa E8 or HPV16 E5 or with the empty vector. Cells were serum starved for 24 h and stimulated with 100 ng of EGF/ml for 10 min, and cell lysates were immunoblotted with an antibody specific for the phosphorylated form of ERK1/2 kinases (p-ERK1/2). The same blot was reprobed with an anti-tubulin antibody to test for equivalent loading. The experiment was performed twice with similar results. (B) Effect of E8 on AP-1 activation. HEK-293T cells were cotransfected with a GFP plasmid and the MMP1-luc reporter plasmid together with CRPVa E8 (E8a), CRPVb E8 (E8b), or HPV16 E5 (16E5) plasmid or with the empty pCiNeo vector (Neo). Cells were serum starved for 24 h and treated overnight with 20 ng of EGF/ml to allow for reporter gene expression. The luciferase activity was normalized to GFP fluorescence of lysates. Relative luciferase activity is normalized to the value obtained in vector-transfected cells with no EGF stimulation. The data represent the mean values and the standard deviations of at least three independent triplicate experiments.

contrast, coexpression of ZnT1 $_{\Delta 1-177}$ and E8 dramatically decreased EGF-mediated AP-1 activation, down to the level observed in the absence of E8 (Fig. 8A). These findings support the notion that the interaction of E8 with endogenous ZnT1 is required for the upregulation of EGFR signaling.

Previous reports showed that the EGF receptor and its signal transducers were rapidly translocated to early endosomes after ligand treatment and that EGFR-containing endosomes served as major sites of generation for persistent signaling through the Ras pathway (35). Since our results showed that E8-ZnT1 interaction was required for EGFR signaling upregulation and that a significant fraction of E8 was localized in early endosomes, we sought to determine whether E8 and ZnT1 localized in EGFR-containing endosomes after EGF stimulation. For these colocalization experiments, we used HeLa cells instead of HaCat cells because they internalized EGFR more rapidly and more efficiently upon ligand treatment (our unpublished observations). HeLa cells contain integrated HPV18 sequences but do not express E5-encoding transcripts (55).

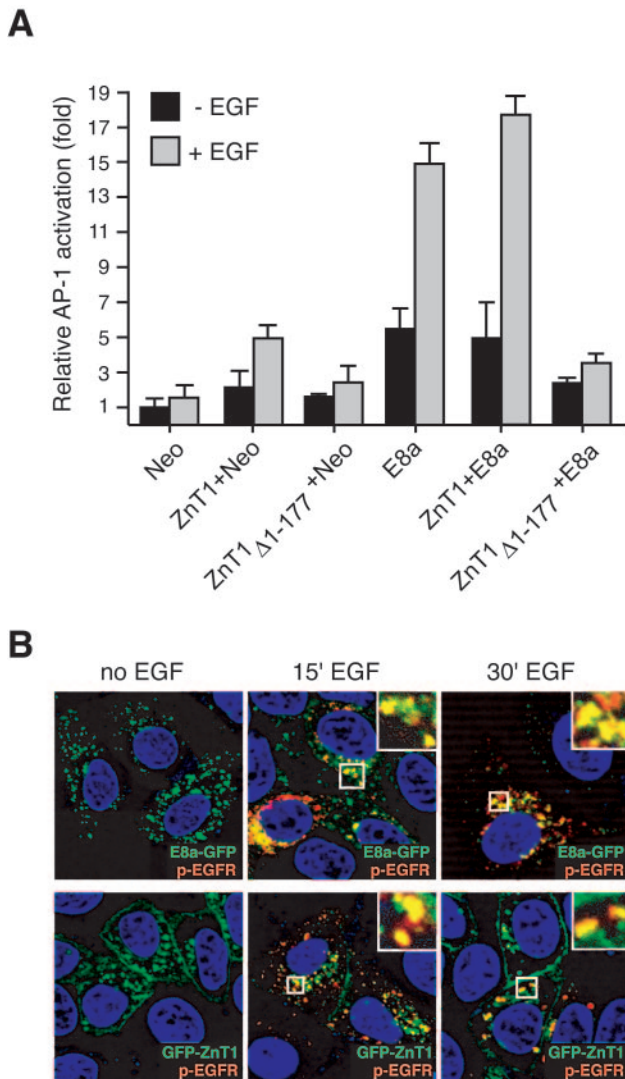


FIG. 8. Requirement for E8-ZnT1 interaction in EGFR signaling activation. (A) Effect of a nonfunctional ZnT1 protein on E8-dependent AP-1 activation. HEK-293T cells were cotransfected with MMP1-luc reporter plasmid and CRPVa E8 plasmid (E8a) and with pCiNeo vectors encoding either full-length ZnT1 or a truncated nonfunctional ZnT1 protein lacking the amino acids 1 to 177 (ZnT1 Δ 1-177). EGF treatment and AP-1 reporter luciferase assay were performed as described in Fig. 7B. (B) Colocalization of E8 or ZnT1 with the EGFR signal transduction complex. HeLa cells were cotransfected with E8a-GFP (upper panels) or GFP-ZnT1 (lower panels) plasmid, together with the pRK5-EGFR construct encoding native human EGFR (32). Cells were serum starved for 24 h, stimulated with EGF for 5 min on ice, and chased for 15 or 30 min or left untreated. Activated EGFR was visualized by indirect immunofluorescence with anti-p-EGFR antibody, and nuclei were stained with DAPI. The figure shows the merged images of green fluorescence (ZnT1 or E8a) and red fluorescence (p-EGFR) obtained with a Zeiss Apo Tome device. Microscope settings were the same in all experiments. Insets show higher magnifications of boxed areas.

Cells were cotransfected with an EGFR expression vector together with E8-GFP or GFP-ZnT1 plasmid. Cells were treated with EGF for 5 min on ice and transferred at 37°C for 15 or 30 min before fixation. The active phosphorylated form of EGFR was revealed by immunofluorescence with a phospho-EGFR

specific antibody, followed by a Cy3-conjugated secondary antibody. No red staining was observed in untreated cells, assessing the specificity of the antibody for the activated receptor (Fig. 8B, left panels). A significant fraction of each of E8-GFP or GFP-ZnT1 colocalized with activated EGFR in small peripheral endocytic vesicles 15 min after ligand treatment (Fig. 8B, middle panels). Colocalization of both proteins with activated EGFR was still observed 30 min after ligand treatment in larger perinuclear vesicles, suggesting that E8-ZnT1 complexes remain associated with the EGFR signaling complex along the endocytic pathway. Together, our data strongly suggest that the interaction of CRPV E8 with ZnT1 upregulates the EGFR signaling cascade generated from the endosomal compartment.

DISCUSSION

The CRPV E8 ORF encodes a short hydrophobic protein with structural features similar to the E5 transmembrane protein encoded by mucosal HPV genotypes (19, 28, 31, 51). The precise function of these proteins in vivo remains largely unknown. We report here that E8 plays a central role in CRPV biology, and we identify several E8 cellular targets that provide novel insights into viral pathogenesis.

CRPV E8, a potent growth-promoting factor for keratinocytes in vivo. Abrogation of the CRPVa or CRPVb E8 start codon resulted in a dramatic decrease in the rate of papilloma formation. This is in contrast with the previous finding that E8 was dispensable for wart induction (34). This apparent discrepancy likely results from different experimental procedures. In our study, viral DNA was inoculated by a bioblastic method without skin pretreatment. In the experiments of Hu et al. (34), skin was chemically pretreated and scarified prior to DNA inoculation, which increases the susceptibility to CRPV infection (23). The resulting epidermal hyperplasia and wound healing involve the release of the slow-cycling, self-renewing epidermal stem cells from the tight microenvironmental control that ensures the homeostasis of the epidermis (1, 61). Epidermal stem cells are the likely primary targets of CRPV infection (54). It may be assumed that the function of E8 is to trigger the proliferation of quiescent epidermal stem cells and that experimentally induced epidermal hyperplasia and wound healing may allow papilloma induction by E8(-) mutants by substituting for E8 function.

We also found that E8 was essential for papilloma growth, in agreement with Hu et al. (34). In papillomas induced by E8(-) genomes we found no evidence for a transcriptional downregulation of E6 and E7 oncogenes, which are required for papilloma formation (63). These findings indicate that sustained expression of E6 and E7 oncogenes is not sufficient for proper papilloma growth and that E8 acts on its own as a potent growth-promoting factor for epidermal cells.

CRPV E8 cellular partners, novel targets in viral pathogenesis. To our knowledge, no systematic screening for the identification of E8- or E5-interacting proteins has been reported thus far. Using an exhaustive yeast two-hybrid screen, we found that CRPV E8 could directly interact with at least three cellular proteins, ZnT1, PCDH1, and AHNAK/desmoyokin. None of the E8-interacting clones corresponded to the 16-kDa subunit of the vacuolar H⁺-ATPase (V-ATPase), a protein previously

shown to interact with HPV16 and HPV6 E5 in coimmunoprecipitation assays (15). Binding of E5 to the V-ATPase mostly relies on hydrophobic transmembrane interactions (26), and it cannot be ruled out that such interactions may not be easily detected by standard two-hybrid assay (58). It would be worth testing for the interaction between CRPV E8 and the 16-kDa V-ATPase subunit by both coimmunoprecipitation and pairwise two-hybrid assays. Most interestingly, we found that HPV16 E5 could also interact with ZnT1, PCDH1, and AHNAK in a two-hybrid assay, which raises the possibility that CRPV E8 and HPV16 E5 proteins exert similar biological functions. The biological significance of these interactions is elusive, since the roles of ZnT1, PCDH1, and AHNAK in skin homeostasis and their possible functional relationship remain to be elucidated.

A first step toward understanding E8 functions. ZnT1 was first identified as a zinc transporter involved in zinc efflux (48) and was found to be essential for early embryonic development in the mouse (2). Zinc plays essential structural and catalytic roles in almost all aspects of cell metabolism (16), and it may be expected that E8-ZnT1 interaction affects several unrelated cellular functions by interfering with zinc transport. Recent studies indicate that the *Caenorhabditis elegans* homologue of ZnT1, the cation diffusion facilitator 1 (CDF-1), is a positive modulator of EGFR signaling in vulval development (11, 36). We found that CRPV E8 increased the phosphorylation of the ERK1/2 MAPK and the activity of Jun/Fos AP-1 complexes upon EGF stimulation, as previously reported for the HPV16 E5 protein (7, 12, 14, 40). Our competition experiments provided strong evidence for the requirement of E8-ZnT1 interaction in AP-1 activation, and our colocalization studies showed that both E8 and ZnT1 colocalized with EGFR signaling complexes in endosomes. However, the precise molecular mechanism by which ZnT1 modulates EGFR signaling remains to be determined. CRPV E8 also induced a moderate activation of AP-1 without EGF treatment, which suggests that E8 and E5 can constitutively activate an EGF-independent signaling pathway leading to AP-1 activation, the nature of which remains to be elucidated. Constitutive activation of AP-1 is sufficient for the induction of skin papillomas in mice (for a review, see reference 3). It is thus likely that EGFR-dependent AP-1 activation by CRPV E8 exerts a crucial role in the induction of skin warts. Consistent with this hypothesis, recent studies indicate that EGFR is required for the induction of epidermal hyperplasia in HPV16 E5 transgenic mice (25). However, these results rely on overexpression experiments, and further studies are needed to find out whether physiological levels of E8 can efficiently modulate EGFR signaling and AP-1 activity in vivo. It should be stressed that the transformation of fibroblastic cells by BPV1 E5 involves the constitutive activation of another tyrosine kinase receptor, the PDGF receptor (33). PDGF receptor is abundantly expressed in fibroblasts and mesenchymal cells but normally not in keratinocytes (20).

Our experiments provided the first experimental evidence for an interaction between ZnT1 and PCDH1 transmembrane proteins and E8 was found to disrupt this interaction. Whether this accounts for the modulation of EGFR signaling via ZnT1 remains to be determined. PCDH1 shares 70% identical amino acids with the *Xenopus laevis* paraxial protocadherin, which functionally interacts with the Wnt pathway and inhibits Rac1

activity in *Xenopus* embryo (60). Since Wnt signaling and Rac1 are critical regulators of epidermal stem cells self-renewal (1, 5), E8-PCDH1 interaction may contribute to the dysregulation of skin homeostasis by interfering with the Wnt pathway and disconnect infected keratinocytes from the growth-inhibitory signals of neighboring cells.

We found no evidence for interaction between AHNAK and PCDH1 or ZnT1. AHNAK was first identified as desmoyokin, a keratinocyte nondesmosomal plaque protein (41), but its role in skin homeostasis remains to be determined (38). AHNAK central repeated units were recently found to mediate the activation of phospholipase C-gamma 1 through protein kinase C (39). Our data indicate that E8 binds several AHNAK CRUs, rendering possible that E8 modulates membrane phospholipid signaling, as previously reported for the HPV16 E5 protein (17).

E5 and E8, major players in HPV pathogenesis? CRPV E8 provides an essential function in papilloma formation and growth, most likely by promoting stem cell proliferation. The striking structural similarities and the common cellular targets of CRPV E8 and HPV16 E5 suggest that HPV E5 proteins should exert a crucial role in the induction of genital warts and squamous intraepithelial lesions. Papillomas can be efficiently induced by HPV16 DNA in human foreskin xenografts (8). It would be of particular interest to investigate the role of HPV16 E5 in vivo using this model.

Canonical E5 ORF is a specific feature of mucosal HPVs of the alpha-genus (19), and most cutaneous HPVs lack a bona fide E5 ORF. However, as-yet-unrecognized E8 ORFs, with coding potential for small hydrophobic proteins, are present in the E6 region of cutaneous HPVs associated with skin warts, including mu-HPV types 1 and 63 and gamma-HPV types 4 and 65 (unpublished observations). In view of our data, it is tempting to speculate that these putative E8 proteins exert a major role in wart formation in humans.

Neither the E5 nor the E8 ORF is found in beta-HPV genotypes, comprising HPV5 and the other genotypes associated with epidermodysplasia verruciformis. Consistent with a role of E5/E8 proteins in lesion formation, EV-HPVs induce only latent infections in the general population (4), and antibodies to HPV5 capsid proteins are only detected upon epidermal repair processes (21). EV lesions occur in individuals carrying homozygous truncating mutations in either *EVER1* or *EVER2* genes, encoding transmembrane proteins with unknown function (49). This could suggest that the inactivation of *EVER1* or *EVER2* gene complements for the lack of E5/E8 proteins in the induction of EV lesions. Experiments are currently in progress to address this issue (M. Favre, Y. Jacob, J. Mendoza, and P. Cassonnet, unpublished data). Advances in the characterization of papillomavirus E5 and E8 proteins should thus provide us with new insights into the biology of HPVs and keratinocytes and open new avenues for therapeutic approaches.

ACKNOWLEDGMENTS

We are grateful to Richard D. Palmiter (University of Washington, Seattle, WA), Jacopo Meldolesi (San Raffaele Scientific Institute, Milan, Italy), and Christophe Lamaze (Institut Curie, Paris, France) for helpful advice. We thank Eleonore Real and Odile Croissant for suggestions and discussion and Patricia Flamant and Christian Pons for technical assistance. We acknowledge Pascal Roux and Emmanuelle

Perret (Institut Pasteur, Paris, France) for technical expertise in confocal microscopy.

M.N. was funded by doctoral fellowships from the Association pour la Recherche contre le Cancer and the Fondation pour la Recherche Médicale, and J.S. was the recipient of a Pasteur-Weizmann fellowship.

REFERENCES

- Alonso, L., and E. Fuchs. 2003. Stem cells of the skin epithelium. *Proc. Natl. Acad. Sci. USA* **100**:11830–11835.
- Andrews, G. K., H. Wang, S. K. Dey, and R. D. Palmiter. 2004. Mouse zinc transporter 1 gene provides an essential function during early embryonic development. *Genesis* **40**:74–81.
- Angel, P., A. Szabowski, and M. Schorpp-Kistner. 2001. Function and regulation of AP-1 subunits in skin physiology and pathology. *Oncogene* **20**:2413–2423.
- Antonsson, A., O. Forslund, H. Ekberg, G. Sterner, and B. G. Hansson. 2000. The ubiquity and impressive genomic diversity of human skin papillomaviruses suggest a commensal nature of these viruses. *J. Virol.* **74**:11636–11641.
- Benitah, S. A., M. Frye, M. Glogauer, and F. M. Watt. 2005. Stem cell depletion through epidermal deletion of Rac1. *Science* **309**:933–935.
- Boussif, O., F. Lezoualc'h, M. A. Zanta, M. D. Mergny, D. Scherman, B. Demeneix, and J. P. Behr. 1995. A versatile vector for gene and oligonucleotide transfer into cells in culture and in vivo: polyethylenimine. *Proc. Natl. Acad. Sci. USA* **92**:7297–7301.
- Bouvard, V., G. Matlashewski, Z. M. Gu, A. Storey, and L. Banks. 1994. The human papillomavirus type 16 E5 gene cooperates with the E7 gene to stimulate proliferation of primary cells and increases viral gene expression. *Virology* **203**:73–80.
- Brandsma, J. L., D. G. Brownstein, W. Xiao, and B. J. Longley. 1995. Papilloma formation in human foreskin xenografts after inoculation of human papillomavirus type 16 DNA. *J. Virol.* **69**:2716–2721.
- Brandsma, J. L., Z.-H. Yang, D. DiMaio, S. W. Barthold, E. Johnson, and W. Xiao. 1992. The putative E5 open reading frame of cottontail rabbit papillomavirus is dispensable for papilloma formation in domestic rabbits. *J. Virol.* **66**:6204–6207.
- Breitbart, F., M. Nonnenmacher, J. Salmon, and G. Orth. 2006. Rabbit viral papillomas and carcinomas: model diseases for human papillomavirus infections and associated carcinogenesis. p. 399–420. *In* S. Campo (ed.), *Papillomavirus research: from natural history to vaccines and beyond*. Caister Academic Press, Norwich, United Kingdom.
- Bruinsma, J. J., T. Jirakulaporn, A. J. Muslin, and K. Kornfeld. 2002. Zinc ions and cation diffusion facilitator proteins regulate Ras-mediated signaling. *Dev. Cell* **2**:567–578.
- Cartin, W., and A. Alonso. 2003. The human papillomavirus HPV2a E5 protein localizes to the Golgi apparatus and modulates signal transduction. *Virology* **314**:572–579.
- Chang, J. L., Y. P. Tsao, D. W. Liu, S. J. Huang, W. H. Lee, and S. L. Chen. 2001. The expression of HPV-16 E5 protein in squamous neoplastic changes in the uterine cervix. *J. Biomed. Sci.* **8**:206–213.
- Chen, S. L., Y. P. Tsao, C. M. Yang, Y. K. Lin, C. H. Huang, and S. W. Kuo. 1995. Differential induction and regulation of c-jun, junB, junD, and c-fos by human papillomavirus type 11 E5a oncoprotein. *J. Gen. Virol.* **76**:2653–2659.
- Conrad, M., V. J. Bubbs, and R. Schlegel. 1993. The human papillomavirus type 6 and 16 E5 proteins are membrane-associated proteins which associate with the 16-kilodalton pore-forming protein. *J. Virol.* **67**:6170–6178.
- Cousins, R. J. 1998. A role of zinc in the regulation of gene expression. *Proc. Nutr. Soc.* **57**:307–311.
- Crusius, K., M. Kaszkin, V. Kinzel, and A. Alonso. 1999. The human papillomavirus type 16 E5 protein modulates phospholipase C-gamma-1 activity and phosphatidylinositol turnover in mouse fibroblasts. *Oncogene* **18**:6714–6718.
- Danos, O., E. Georges, G. Orth, and M. Yaniv. 1985. Fine structure of the cottontail rabbit papillomavirus mRNAs expressed in the transplantable VX2 carcinoma. *J. Virol.* **53**:735–741.
- de Villiers, E. M., C. Fauquet, T. R. Broker, H. U. Bernard, and H. zur Hausen. 2004. Classification of papillomaviruses. *Virology* **324**:17–27.
- DiMaio, D., and D. Mattoon. 2001. Mechanisms of cell transformation by papillomavirus E5 proteins. *Oncogene* **20**:7866–7873.
- Favre, M., S. Majewski, B. Noszczyk, F. Maienfisch, A. Pura, G. Orth, and S. Jablonska. 2000. Antibodies to human papillomavirus type 5 are generated in epidermal repair processes. *J. Invest. Dermatol.* **114**:403–407.
- Frank, M., and R. Kemler. 2002. Protocadherins. *Curr. Opin. Cell Biol.* **14**:557–562.
- Friedewald, W. F. 1942. Cell state as affecting susceptibility to a virus. Enhanced effectiveness of the rabbit papillomavirus on hyperplastic epidermis. *J. Exp. Med.* **75**:197–219.
- Fromont-Racine, M., J. C. Rain, and P. Legrain. 1997. Toward a functional analysis of the yeast genome through exhaustive two-hybrid screens. *Nat. Genet.* **16**:277–282.
- Genther Williams, S. M., G. L. Disbrow, R. Schlegel, D. Lee, D. W. Threadgill, and P. F. Lambert. 2005. Requirement of epidermal growth factor receptor for hyperplasia induced by e5, a high-risk human papillomavirus oncogene. *Cancer Res.* **65**:6534–6542.
- Gieswein, C. E., F. J. Sharom, and A. G. Wildeman. 2003. Oligomerization of the E5 protein of human papillomavirus type 16 occurs through multiple hydrophobic regions. *Virology* **313**:415–426.
- Gietz, R. D., R. H. Schiestl, A. R. Willems, and R. A. Woods. 1995. Studies on the transformation of intact yeast cells by the LiAc/SS-DNA/PEG procedure. *Yeast* **11**:355–360.
- Giri, I., O. Danos, and M. Yaniv. 1985. Genomic structure of the cottontail rabbit (Shope) papillomavirus. *Proc. Natl. Acad. Sci. USA* **82**:1580–1584.
- Han, R., F. Breitbart, P. N. Marche, and G. Orth. 1992. Linkage of regression and malignant conversion of rabbit viral papillomas to MHC class II genes. *Nature* **356**:66–68.
- Han, R., N. M. Cladel, C. A. Reed, and N. D. Christensen. 1998. Characterization of transformation function of cottontail rabbit papillomavirus E5 and E8 genes. *Virology* **251**:253–263.
- Harry, J. B., and F. O. Wettstein. 1996. Transforming properties of the cottontail rabbit papillomavirus oncoproteins LE6 and SE6 and of the E8 protein. *J. Virol.* **70**:3355–3362.
- Herbst, R., R. Lammers, J. Schlessinger, and A. Ullrich. 1991. Substrate phosphorylation specificity of the human c-kit receptor tyrosine kinase. *J. Biol. Chem.* **266**:19908–19916.
- Howley, P. M., and D. R. Lowy. 2001. Papillomaviruses and their replication, p. 2197–2330. *In* D. M. Knipe, P. M. Howley, D. E. Griffin, R. A. Lamb, M. A. Martin, B. Roizman, and S. E. Straus (ed.), *Fields virology*, 4th ed., vol. 2. Lippincott/The Williams & Wilkins Co., Philadelphia, Pa.
- Hu, J., R. Han, N. M. Cladel, M. D. Pickel, and N. D. Christensen. 2002. Intracutaneous DNA vaccination with the E8 gene of cottontail rabbit papillomavirus induces protective immunity against virus challenge in rabbits. *J. Virol.* **76**:6453–6459.
- Jiang, X., and A. Sorkin. 2002. Coordinated traffic of Grb2 and Ras during epidermal growth factor receptor endocytosis visualized in living cells. *Mol. Biol. Cell* **13**:1522–1535.
- Jirakulaporn, T., and A. J. Muslin. 2004. Cation diffusion facilitator proteins modulate Raf-1 activity. *J. Biol. Chem.* **279**:27807–27815.
- Jonat, C., B. Stein, H. Ponta, P. Herrlich, and H. J. Rahmsdorf. 1992. Positive and negative regulation of collagenase gene expression. *Matrix Suppl.* **1**:145–155.
- Kouno, M., G. Kondoh, K. Horie, N. Komazawa, N. Ishii, Y. Takahashi, J. Takeda, and T. Hashimoto. 2004. Ahnak/Desmoyokin is dispensable for proliferation, differentiation, and maintenance of integrity in mouse epidermis. *J. Invest. Dermatol.* **123**:700–707.
- Lee, I. H., J. O. You, K. S. Ha, D. S. Bae, P. G. Suh, S. G. Rhee, and Y. S. Bae. 2004. AHNAK-mediated activation of phospholipase C-gamma1 through protein kinase C. *J. Biol. Chem.* **279**:26645–26653.
- Leechanchai, P., L. Banks, F. Moreau, and G. Matlashewski. 1992. The E5 gene from human papillomavirus type 16 is an oncogene which enhances growth factor-mediated signal transduction to the nucleus. *Oncogene* **7**:19–25.
- Masunaga, T., H. Shimizu, A. Ishiko, T. Fujiwara, T. Hashimoto, and T. Nishikawa. 1995. Desmoyokin/AHNAK protein localizes to the non-desmosomal keratinocyte cell surface of human epidermis. *J. Invest. Dermatol.* **104**:941–945.
- McMahon, R. J., and R. J. Cousins. 1998. Regulation of the zinc transporter ZnT-1 by dietary zinc. *Proc. Natl. Acad. Sci. USA* **95**:4841–4846.
- McMichael, H. 1967. Inhibition by methylprednisolone of regression of the Shope rabbit papilloma. *J. Natl. Cancer Inst.* **39**:55–65.
- Münger, K., and P. M. Howley. 2002. Human papillomavirus immortalization and transformation functions. *Virus Res.* **89**:213–228.
- Nie, Z., W. Ning, M. Amagai, and T. Hashimoto. 2000. C-Terminus of desmoyokin/AHNAK protein is responsible for its translocation between the nucleus and cytoplasm. *J. Invest. Dermatol.* **114**:1044–1049.
- Oetke, C., E. Auvinen, M. Pawlita, and A. Alonso. 2000. Human papillomavirus type 16 E5 protein localizes to the Golgi apparatus but does not grossly affect cellular glycosylation. *Arch. Virol.* **145**:2183–2191.
- Orth, G. 1987. Epidermodysplasia verruciformis, p. 199–243. *In* P. M. Howley and N. P. Salzman (ed.), *The papillomaviruses*, vol. 2. Plenum Press, Inc., New York, N.Y.
- Palmiter, R. D., and S. D. Findley. 1995. Cloning and functional characterization of a mammalian zinc transporter that confers resistance to zinc. *EMBO J.* **14**:639–649.
- Ramoz, N., L.-A. Rueda, B. Bouadjar, L.-S. Montoya, G. Orth, and M. Favre. 2002. Mutations in two adjacent novel genes are associated with epidermodysplasia verruciformis. *Nat. Genet.* **32**:553–561.
- Rous, P., and J. W. Beard. 1935. The progression to carcinoma of virus-induced rabbit papillomas (Shope). *J. Exp. Med.* **62**:523–548.
- Salmon, J., M. Nonnenmacher, S. Cazé, P. Flamant, O. Croissant, G. Orth, and F. Breitbart. 2000. Variation in the nucleotide sequence of cottontail rabbit papillomavirus a and b subtypes affects wart regression and malignant

- transformation and the level of viral replication in domestic rabbits. *J. Virol.* **74**:10766–10777.
52. **Salmon, J., N. Ramoz, P. Cassonnet, G. Orth, and F. Breitburd.** 1997. A cottontail rabbit papillomavirus strain (CRPVb) with strikingly divergent E6 and E7 oncoproteins: an insight in the evolution of papillomaviruses. *Virology* **235**:228–234.
 53. **Sano, K., H. Tanihara, R. L. Heimark, S. Obata, M. Davidson, T. St John, S. Taketani, and S. Suzuki.** 1993. Protocadherins: a large family of cadherin-related molecules in central nervous system. *EMBO J.* **12**:2249–2256.
 54. **Schmitt, A., A. Rochat, R. Zeltner, L. Borenstein, Y. Barrandon, F. O. Wettstein, and T. Iftner.** 1996. The primary target cells of the high-risk cottontail rabbit papillomavirus colocalize with hair follicle stem cells. *J. Virol.* **70**:1912–1922.
 55. **Schneider-Gadicke, A., and E. Schwarz.** 1986. Different human cervical carcinoma cell lines show similar transcription patterns of human papillomavirus type 18 early genes. *EMBO J.* **5**:2285–2292.
 56. **Shtivelman, E., and J. M. Bishop.** 1993. The human gene AHNAK encodes a large phosphoprotein located primarily in the nucleus. *J. Cell Biol.* **120**: 625–630.
 57. **Shtivelman, E., F. E. Cohen, and J. M. Bishop.** 1992. A human gene (AHNAK) encoding an unusually large protein with a 1.2-microns polyionic rod structure. *Proc. Natl. Acad. Sci. USA* **89**:5472–5476.
 58. **Stagljar, I., and S. Fields.** 2002. Analysis of membrane protein interactions using yeast-based technologies. *Trends Biochem. Sci.* **27**:559–563.
 59. **Suzuki, S. T.** 2000. Recent progress in protocadherin research. *Exp. Cell Res.* **261**:13–18.
 60. **Unterseher, F., J. A. Hefele, K. Giehl, E. M. De Robertis, D. Wedlich, and A. Schambony.** 2004. Paraxial protocadherin coordinates cell polarity during convergent extension via Rho A and JNK. *EMBO J.* **23**:3259–3269.
 61. **Watt, F. M.** 2002. Role of integrins in regulating epidermal adhesion, growth and differentiation. *EMBO J.* **21**:3919–3926.
 62. **Wettstein, F. O.** 1990. State of viral DNA and gene expression in benign versus malignant tumors, p. 155–179. *In* H. Pfister (ed.), *Papillomaviruses and human cancer*. CRC Press, Inc., Boca Raton, Fla.
 63. **Wu, X., W. Xiao, and J. L. Brandsma.** 1994. Papilloma formation by cottontail rabbit papillomavirus requires E1 and E2 regulatory genes in addition to E6 and E7 transforming genes. *J. Virol.* **68**:6097–6102.
 64. **zur Hausen, H.** 2001. Cervical carcinoma and human papillomavirus: on the road to preventing a major human cancer. *J. Natl. Cancer Inst.* **93**:252–253.